coatings

MDPI

Article

Photocatalytic Inactivation of *Bacillus subtilis* Spores by Natural Sphalerite with Persulfate under Visible Light Irradiation

Yan Liu [1], Zhenni Liu [1], Dong Liu [2] and Wanjun Wang [1,*]

[1] Guangzhou Key Laboratory of Environmental Catalysis and Pollution Control, Institute of Environmental Health and Pollution control, School of Environmental Science and Engineering, Guangdong University of Technology, Guangzhou 510060, China; 2111907012@mail2.gdut.edu.cn (Y.L.); 2112107114@mail2.gdut.edu.cn (Z.L.)

[2] College of Materials Science and Engineering, Shenzhen University, Shenzhen 518000, China; dongliu@szu.edu.cn

* Correspondence: wanjun@gdut.edu.cn

Abstract: Bacterial spores are highly resistant to be inactivated by conventional water disinfection methods. In this study, the inactivation efficiency and mechanisms of *Bacillus subtitles* (*B. subtilis*) spores by natural sphalerite (NS) with persulfate (PS) under visible light (Vis) irradiation were investigated for the first time. The NS was composed of ZnS doped with trace amounts of metal ions, including As, Fe, Cd, and Mn. The results showed that 7 log of *B. subtilis* spores could be completely inactivated within 5 h in the Vis/NS/PS photocatalytic system, and the inactivation efficiency was about four and seven times higher than that of the NS/PS system and the Vis/PS system, respectively. The photo-generated electrons are generated by the excitation of NS under the illumination activated PS to form PS radicals ($\cdot SO_4^-$) and hydroxyl radicals (·OH), which are the main active species for spore inactivation. Mechanism studies further showed that spore inactivation was related to physiological responses, including the increase in intracellular reactive oxygen species, the change of induced antioxidant enzyme activity, and the change of total protein. Furthermore, the dynamic changes of cells during spore inactivation were observed by SEM. These results not only clarify the relationship between the cell physiological stress response and inactivation mechanism of spores, but also reveal the interaction between minerals and PS under Vis, which provides technical methods for the inactivation of bacterial spores in the field of water disinfection.

Keywords: photocatalysis; bacterial spores; persulfate; natural sphalerite; visible light

check for updates

Citation: Liu, Y.; Liu, Z.; Liu, D.; Wang, W. Photocatalytic Inactivation of *Bacillus subtilis* Spores by Natural Sphalerite with Persulfate under Visible Light Irradiation. *Coatings* **2022**, *12*, 528. https://doi.org/10.3390/coatings12040528

Academic Editor: Aivaras Kareiva

Received: 27 March 2022
Accepted: 11 April 2022
Published: 13 April 2022

Publisher's Note: MDPI stays neutral with regard to jurisdictional claims in published maps and institutional affiliations.

Copyright: © 2022 by the authors. Licensee MDPI, Basel, Switzerland. This article is an open access article distributed under the terms and conditions of the Creative Commons Attribution (CC BY) license (https://creativecommons.org/licenses/by/4.0/).

1. Introduction

Water-borne diseases are generally transmitted through microorganisms, such as viruses, bacteria, and protozoa [1]. According to the United Nations Environment and Development Program, about 80% of human diseases are related to bacterial infections, and more than 60% of these diseases are transmitted through drinking water. Among these microbial pollutants, *Bacillus* has the ability to produce a large number of dormant spores. Spores can resist harsh environments and are highly tolerant to heat, alkali, acid, high permeability, and radiation. Once the spore is exposed to a more favorable environment, it can resume the growth process and potentially contribute to the spread of waterborne diseases [2]. Therefore, developing cost-effective methods for the inactivation of bacterial spores is of major importance and has become one of the research hotspots in recent years.

However, according to the current research reports, there continue to be many deficiencies in the use of traditional disinfection techniques to inactivate spores. For example, chlorine disinfection has a very limited inactivation effect on spores. In addition, ozone disinfection is expensive [3], and ultraviolet disinfection has no continuous disinfection

function and limited inactivation effect [4]. These conventional disinfection techniques not only fail to inactivate spores quickly and efficiently, but also require high costs. At the same time, intermediates may also be generated during the disinfection process, resulting in secondary pollution of the environment. Fortunately, photocatalytic disinfection technology achieves the effective inactivation of pathogenic microorganisms in water by using solar energy as an energy source to generate highly reactive oxygen species, such as hydroxyl radicals (·OH), etc. [5,6]. This technology has the advantages of low energy consumption, strong oxidizing power, and fewer disinfection by-products [7]. Photocatalytic disinfection technology has been successfully used to inactivate various conventional non-spore-producing pathogens, such as *Escherichia coli (E. coli)* [8], *Pseudomonas aeruginosa* [9], and *Staphylococcus aureus* [10], but the inactivation efficiency of bacterial spores with a dense spore coat and cortex is still relatively limited. A large number of studies have mainly focused on the inactivation of *Bacillus* vegetative cells by photocatalytic technology, while the research on the dormant spores formed by *Bacillus* is very limited. Ghodsi et al. studied the efficiency of the photocatalytic inactivation of *Bacillus* vegetative cells using g-C_3N_4/Fe_3O_4/Ag nanocomposites [11]. Li and Su et al. synthesized metal-doped (i.e., Pt, Ag) TiO_2 to inactivate spores under ultraviolet (UV) light [12,13]. However, almost all the catalysts used in the spore inactivation were artificially synthesized catalysts, which suffered from the disadvantages of high cost, cumbersome preparation, and inability to utilize visible light.

In recent years, some natural minerals with semiconductor properties have been found to have photocatalytic properties, which can achieve the organic degradation and inactivation of some bacteria [14,15]. These natural catalysts have the advantages of low costs and can be obtained in a large quantity (in tons of scale). Chen et al. used natural sphalerite (NS) driven by Vis to inactivate 7 log Gram-negative *E. coli* [16]. Moradi et al. evaluated the ability to inactivate *E. coli* using oxalate-natural pyrite under visible light [17]. In addition, Peng et al. utilized natural magnetic sphalerite to effectively inactivate the Gram-positive bacterium *Bacillus subtitles* (*B. subtilis*) in a photocatalytic system [18]. However, whether natural mineral catalysts can be used in pure bacterial spore inactivation is still unknown.

In addition, persulfate (PS)-based advanced oxidation process has been widely used in wastewater treatment. PS can be activated to form $\cdot SO_4^-$ under certain conditions, which has higher redox potential and stability than ·OH. Therefore, PS has received extensive attention in the field of organic pollutant degradation and disinfection of water [19,20]. For example, Wang et al. used Vis to activate PS to inactivate *E. coli* [19]. In addition, Latif et al. studied Fe^{2+} to activate peroxymonosulfate (PMS) to produce $\cdot SO_4^-$ to inactivate *E. coli* [21]. It has been reported that in the magnetic hydrochar (MHC)/PS/Vis system, the photogenerated electrons generated by Fe_3O_4 in the composite can activate PS, thereby improving the inactivation efficiency of coliforms [20]. Therefore, to achieve the efficient inactivation of stubborn pathogenic microorganisms such as bacterial spores, it is hypothesized that the oxidation ability of natural mineral photocatalysts could be significantly improved by adding PS. However, to the best of our knowledge, there are no reports on the inactivation of bacterial spores by natural mineral photocatalysts combined with PS addition. Moreover, the biological stress response and inactivation mechanisms of bacterial spores during photocatalytic treatments need to be systematically investigated.

Herein, NS were used to couple with PS under Vis irradiation to construct an advanced water disinfection system, which was applied in the inactivation of *B. subtilis* spores for the first time. The efficiency and feasibility of bacterial spore inactivation were evaluated using the Vis/NS/PS system, which was further improved by optimizing light intensity and temperature. In addition, the mechanisms of bacterial inactivation, major active species, antioxidant enzyme activities, and cell morphological changes were systematically investigated. The research could provide innovative information for the development of low-cost bacterial spore-inactivating natural mineral catalysts, leading to a new "green" water disinfection system utilizing inexhaustible solar energy.

2. Materials and Methods

2.1. Chemicals

Anhydrous ethanol (C_2H_5OH) was purchased from Guangzhou Chemical reagent, China. Nutrition broth (NB) agar was purchased from UK Oxoid. Sodium chloride (NaCl) was purchased from Tianjin Zhiyuan Chemical, China. L-alanine ($C_3H_7NO_2$), potassium persulfate (PS) ($K_2S_2O_8$), anhydrous manganese chloride ($MnCl_2$), calcium chloride ($CaCl_2$), and zinc chloride ($ZnCl_2$) were purchased from Aladdin Reagent, China. All the reagents were of analytical grade and used without further purification.

2.2. Preparation and Characterization of NS Samples

The NS used in the study was collected from Huangshaping deposit in Hunan Province, China. The NS used in this study was mechanically crushed, ground and screened to obtain micron-sized sphalerite powder with particle size less than 40 μm [6,22]. Thus, pure ZnS powders (Sigma, 99.99%) were also used as reference samples. The NS samples were characterized adopting X-ray diffraction (XRD) (Rigaku, Japan, Cu Kα, λ = 0.15406) and the UV-visible diffuse-reflectance spectrum (UV-Vis DRS) (UV-3600 Plus, Shimadzu, Japan) technique to analyze the crystal structure and light absorption performance, respectively. The elemental constitution of NS was analyzed by Inductively Coupled Plasma Mass Spectrometry (ICP-MS) (IAP RQ, Thermo Fishe, Germany) after nitric acid digestion.

2.3. Harvest and Enumeration of Spores

B. subtilis ATCC6633 (Qingdao Hope Biotechnology, Shandong, China) was used as the bacterial strain. To obtain pure spores, bacterial sporulation experiments were carried out. Briefly, *B. subtilis* suspension was placed on NB agar medium containing a certain amount of metal cations and cultured at 37 °C for 4 days. Bacteria were scraped from the agar surface with a sterile curved glass rod and suspended in sterile distilled water. The obtained bacterial suspension was heated at 80 °C for 20 min to remove vegetative cells to obtain spores. Then, the spores were harvested by centrifugation and washing with saline for at least 3 times.

To enumerate the produced spores, samples of the spore suspension were heated in a water bath at 70 °C for 10 min to promote spore germination, and then diluted to the appropriate concentration with 0.85% NaCl. The heat-activated spores were transferred to a NB agar medium containing 10 mM L-alanine to further promote germination, and were finally incubated at 37 °C for 20 h in an incubator (Yiheng, Shanghai, China) for plate counting. Log-reduction was used to describe the inactivation efficiency of spore cells during photocatalytic treatment, which was expressed by the following Equation (1):

$$\text{Log-reduction} = \log_{10} (N_0/N_t) \quad (1)$$

where N_0 was the spore density (colony-forming unit (cfu)/mL) at the initial time zero and N_t was the spore density (cfu/mL) at treatment time t.

To avoid any influence from vegetative cells of *B. subtilis* and obtain 100% of spores, different concentrations of metal cations as sporulation stimulator, including Zn^{2+}, Ca^{2+}, and Mn^{2+}, were added to the NB agar. The sporulation efficiency was determined by counting the spores produced by the above method.

2.4. Photocatalytic Inactivation of Spores

The reactor was open on the top, and a 300 W xenon lamp was installed on the top towards the reactor. To avoid the UV light irradiation, a UV filter (which cuts off light of wavelength below 420 nm, Fuzhe, Shenzhen, China) was equipped on the xenon lamp to obtain visible light (λ > 420 nm). *B. subtilis* spores were diluted with sterile saline to obtain a spore suspension with a concentration of 1×10^7 cfu/mL. 100 mg NS powder and 100 mg PS were added to 50 mL of the above pure spore suspension. The mixed suspension was stirred in the dark for 30 min, and then a light was turned on to initiate the reactions. The

temperature of the reaction vessel (Wolters Kluwer, Yancheng, China) was adjusted to 40 °C. Samples were taken at given time intervals and the number of spores was determined by the method described above.

2.5. Analysis

Intracellular reactive oxygen species (ROS) levels were analyzed using a fluoroacetic acid 2′,7′-dichlorofluorescein diacetate (DCFH-DA) fluorescent probe (S0033, Boyotime, Shanghai, China). A bacterial protein extraction kit (C600596, Sangon Biotech, Shanghai, China) was utilized to extract intracellular enzymatic proteins. The protein concentration, catalase (CAT) activity, and superoxide dismutase (SOD) activity were determined using the modified Bradford protein assay kit (C503041, Sangon Biotech), CAT assay kit (S0051, Boyotime), and SOD assay kit (S0101, Boyotime), respectively. A scanning electron microscope (SEM) (SU8010, Hitachi, Japan) was used to observe the changes of spore morphology during spore inactivation (SEM magnifications are shown in the Figure captions).

3. Results

3.1. Catalyst Characterization

The crystal structure of NS samples was tested by XRD, and the obtained XRD patterns are illustrated in Figure 1a. The XRD pattern of NS shows three main diffraction peaks at 2θ = 28.6°, 2θ = 47.5°, and 2θ = 56.5°, which are consistent with the main diffraction peaks displayed by the standard PDF card of ZnS. It is well known that ZnS is the main component of NS, which is consistent with the XRD pattern. In order to study the light absorption ability of NS, UV-Vis DRS spectroscopy was carried out on pure ZnS and NS powders. As shown in Figure 1b, pure ZnS only exhibits UV-responsive property with light absorption edge below 400 nm, while NS shows extended light absorption up to 800 nm, indicating NS could be excited by almost the whole range of Vis spectrum. The elemental components of NS were further evaluated after digesting powders with nitric acid and determined by ICP. It was found that the digested solution of NS has large amounts of Zn and traces amounts of As, Fe, Cd, and Mn (Figure S1). The weight ratio of each element in NS was calculated to be 90% Zn, 5.2% As, 1.6% Fe, 2.7% Cd, and 0.5% Mn (Table S1). These results indicate that the NS could be regarded as various metal-doped ZnS. Pure ZnS had a band gap of about 3.7 eV, and the absorption edge was about 345 nm, which was only active under UV irradiation [23]. In the case of NS, with the natural doping of metal ions, impurity levels would be formed in the band structure, which extended the absorption edge to the Vis region. This kind of intrinsic doping was provided by nature without artificial synthesis, significantly lowering the costs of large-scale applications. Natural doping in NS leads catalysts to be excited by Vis, which favors the subsequent photocatalytic inactivation of spores.

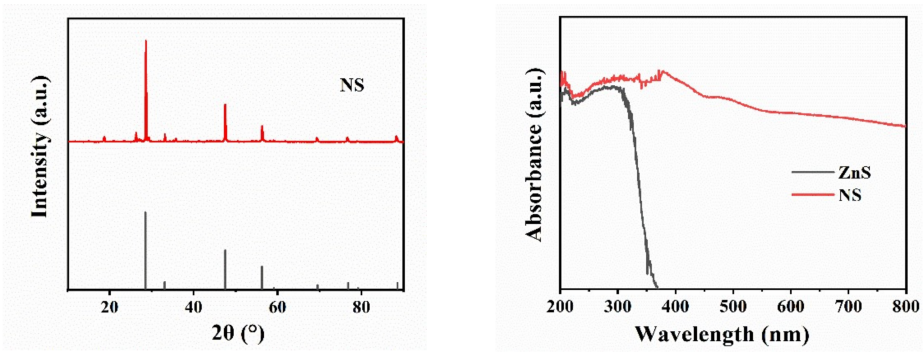

(**a**) (**b**)

Figure 1. (**a**) X-ray diffraction (XRD) patterns of NS; (**b**) UV-visible diffuse-reflectance spectrum (UV-Vis DRS) of pure ZnS and NS.

3.2. Preparation of Pure Bacterial Spores

Previous studies on the inactivation of *B. subtilis* have not ruled out the influence of vegetative cells. To achieve a real inactivation efficiency for pure spores, we first investigated the sporulation by external stimulants and established a method to obtain 100% spores. It has been reported that metal ions, such as Ca^{2+} and Mn^{2+}, could promote the efficiency of sporulation [24,25] while Zn^{2+} may be released from NS. Therefore, Zn^{2+}, Ca^{2+}, and Mn^{2+} were selected to test their ability for spore cultivation in this study. As shown in Figure 2a, the effects of Zn^{2+} ($ZnCl_2$), Ca^{2+} ($CaCl_2$), and Mn^{2+} ($MnCl_2$) on the sporulation efficiency were studied, and it was found that the addition of Zn^{2+} had no effect on the sporulation efficiency, while the addition of Ca^{2+} and Mn^{2+} could significantly improve the sporulation efficiency. Specifically, both Ca^{2+} and Mn^{2+} additions increased the sporulation efficiency by 50% after incubation for 8 h. It was further found that 0.25 g/L Mn^{2+} could obtain 100% sporulation efficiency at six days (Figure S2), which effectively shortened the time period of spore production. Moreover, the addition of 0.5 g/L Ca^{2+} could obtain 100% sporulation efficiency in the shortest four-day period (Figure 2b). This indicates that Ca^{2+} could not only improve the sporulation efficiency, but also shorten the sporulation time. In addition, spore densities of different refined concentrations of Ca^{2+} and Mn^{2+} on the eighth day of culture could be visually observed by SEM (Figure S3). Thus, to obtain pure spores for the tests, the *B. subtilis* was cultured with the addition of 0.5 g/L Ca^{2+} in the NB agar and cultured at 37 °C for four days.

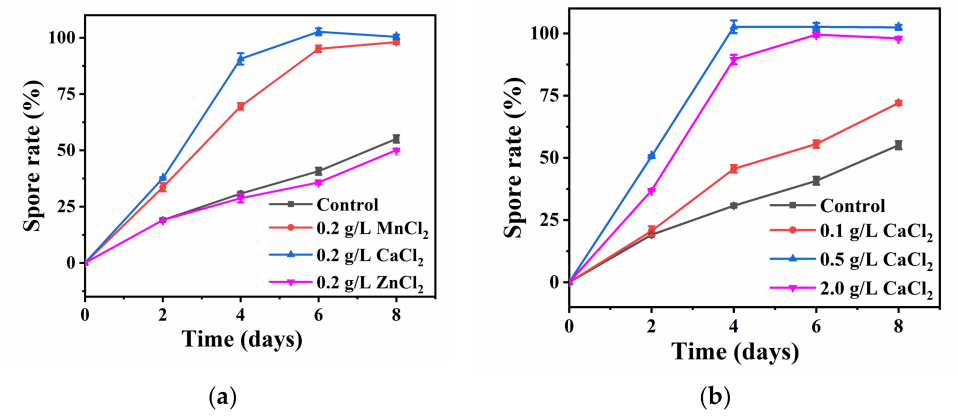

Figure 2. (**a**) Sporulation efficiency of *B. subtilis* with the same concentration of Mn^{2+}, Ca^{2+} and Zn^{2+}; (**b**) Sporulation efficiency of *B. subtilis* with different concentrations of Ca^{2+}.

3.3. Inactivation Efficiency of Spores

The photocatalytic inactivation of pure spores in different systems was compared. As shown in Figure 3, the Vis, Vis/NS, and Vis/PS system has almost no inactivation effect on *B. subtilis* spores, suggesting that the photocatalytic effect of NS and Vis-activated PS could not inactivate bacterial spores. In contrast, bacterial spores of about 1.8 log were inactivated within 6 h in NS/PS system. This may be due to the activation of PS by metal ions of Fe^{2+}, Mn^{2+} released from NS. Interestingly, it was found that in the Vis/NS/PS system, the inactivation efficiency was significantly improved, and all *B. subtilis* spores (7.0 log) were completely inactivated within 5 h. The spore inactivation efficiency of the Vis/NS/PS system was about four and seven times higher than that of the NS/PS system and the Vis/PS system, respectively. It could be estimated that the spore inactivation efficiency in the Vis/NS/PS system was higher than the sum of Vis/NS, Vis/PS, and NS/PS systems. Therefore, this result indicates that there exists a synergistic effect of photocatalysis and PS activation, which leads to the significant enhancement of spore inactivation efficiency. Table 1 compares the current literature regarding the photocatalytic inactivation of bacterial spores. It is noted that among the methods for the inactivation of *B. subtilis* spores, the efficiency in our proposed Vis/NS/PS system is the highest, except for some studies that used Ag/TiO_2 as the photocatalyst, which is expensive and toxic to the environment.

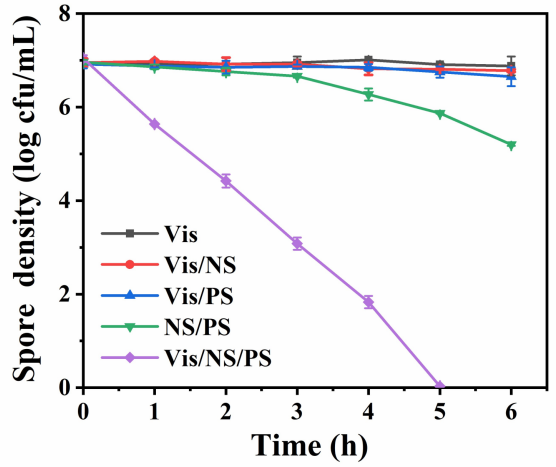

Figure 3. Bacterial spore inactivation efficiency in Vis/NS/PS system and other control systems including Vis, Vis/NS, Vis/PS and NS/PS.

Table 1. Comparison with recent literatures on photocatalytic inactivation of bacterial spores.

Phocatalyst	Bacterial Strains	Light Source	Bacterial Concentration (cfu/mL)	Inactivation Efficiency	Reference
TiO_2	*B. cereus* spores	UV/high pressure	1×10^9	5.0 log-reduction in 1 h (~5 log/h)	[26]
$Ag/Pt/TiO_2$	*B. stearothermophilus* spores	UV-Vis	4×10^7	5.6 log-reduction in 1.5 h (~3.75 log/h)	[27]
TiO_2	*B. anthracis* spores	UV	1×10^4	4.0 log-reduction in 5 h (~0.8 log/h)	[28]
TiO_2	*B. subtilis* spores	UV	1×10^7	7.0 log-reduction in 24 h (~0.29 log/h)	[29]
TiON/PdO	*B. subtilis* spores	/	1×10^6	2.7 log-reduction in 3 h (~0.9 log/h)	[2]
Ag/TiO_2	*B. subtilis* spores	Vis/micro/nano bubble	1×10^5	4.0-reduction log in 1 h (~4 log/h)	[30]
TiO_2	*B. subtilis* spores	UV	1×10^8	6.7 log-reduction in 8 h (~0.84 log/h)	[31]
NS/PS	*B. subtilis* spores	Vis	1×10^7	7.0 log-reduction in 5 h (~1.4 log/h)	This work

To understand the influence of key operational factors on the inactivation efficiency in the Vis/NS/PS system, experiments were conducted with different light intensity and reaction temperature. As shown in Figure 4a, with the increase of light intensity, bacterial spore inactivation efficiency gradually increased. When the light intensity increased to 70 mM/cm^2, the Vis/NS/PS system achieved the highest spore inactivation effect. In addition, as shown in Figure 4b, when the temperature was 20 °C, only 5 log-reduction of spores was achieved within 6 h. With the increase of temperature to 40 °C, the inactivation efficiency was promoted and total inactivation of 7 log spores occurred within 5 h. These results indicate that both light intensity and reaction temperature have positive effects on the photocatalytic spore inactivation in the Vis/NS/PS system.

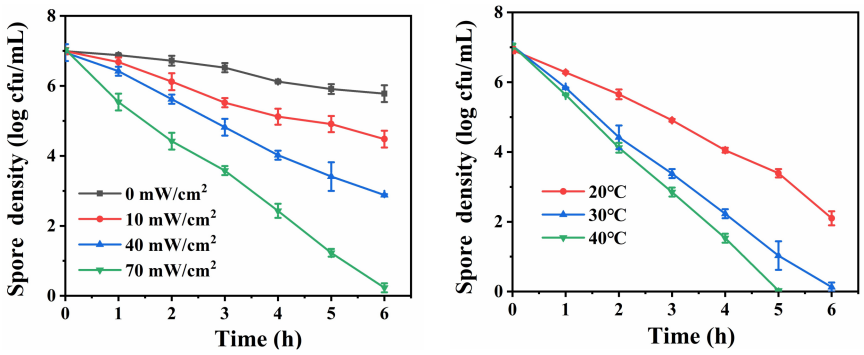

Figure 4. (**a**) Comparison of the efficiency of inactivating bacterial spores under different light intensities (The reaction temperature was kept at 30 °C); (**b**) Comparison of the efficiency of inactivating bacterial spores at different temperatures (The light intensity was kept at 70 mM/cm^2).

3.4. Mechanism of Spore Inactivation

The NS has semiconductor property and could be excited by Vis (Figure 1b). However, the Vis/NS system has limited spore inactivation efficiency (Figure 3). Therefore, PS played a crucial role in the spore inactivation process. According to previous studies, a large number of active species could be generated in the Vis/PS system, including $\cdot SO_4^-$, ·OH, and $\cdot O_2^-$ [19,20]. However, the Vis/PS also exhibited limited spore inactivation efficiency, suggesting the PS was activated by the photocatalytic effect of NS in the present study. It has been reported that the PS could be activated by photo-generated e^- to produce $\cdot SO_4^-$, which could further transform to ·OH [19]. Therefore, it was proposed that the PS in the Vis/NS/PS was also activated by the photo-generated e^- from photo-excited NS, following Equations (2)–(4). The produced $\cdot SO_4^-$ and ·OH were the major reactive species for the inactivation of *B. subtilis* spores.

$$NS \rightarrow e^- + h^+, \quad (2)$$

$$S_2O_8^{2-} + e^- \rightarrow \cdot SO_4^- + OH^-, \quad (3)$$

$$SO_4^- + H_2O \rightarrow SO_4^{2-} + \cdot OH + H^+, \quad (4)$$

Previous studies have demonstrated that oxidative stress exists in the process of bacterial inactivation. For instance, Wang et al. detected a strong oxidative stress response in the process of bacterial inactivation in a photo-Fenton system [32]. However, oxidative stress on spores has not been well understood. To this end, the oxidative stress during spore inactivation was further investigated. It is a known fact that the endogenous damage caused by oxidative stress (intracellular ROSs) may also lead to cellular inactivation. Primarily, the situation of intracellular ROSs was studied by using the fluorescent probe DCFH-DA to detect intracellular ROSs. After DCFH-DA enters the cell, if the cell membrane remains intact, its enzymatic hydrolysis product DCFH could not be released. As shown in Figure 5a, compared with other systems, the intracellular ROSs in the Vis/NS/PS system gradually increased to a maximum value and then decreased with time, indicating that oxidative stress was generated in cells due to membrane damage. This result also indicates that the rapid and large amount of producing $\cdot SO_4^-$ oxidizes the cell membrane. In order to further confirm this statement, the activities of CAT and SOD were also tested. As shown in Figure 5b, the CAT activity increased rapidly to 0.8 U/mg from 0 to 4 h, and the CAT activity decreased gradually to 0.6 U/mg from 4 to 6 h over time, indicating a strong oxidative stress reaction in spores. The increase of CAT activity indicated the triggering of biological stress responses, while the decrease of CAT activity suggested that the bacterial defense system was destructive. Compared with Vis, Vis/PS, and NS/PS, the Vis/NS/PS system has higher CAT activity, indicating that the Vis/NS/PS system has intense oxidative stress and played a positive role in spore inactivation. To further illustrate the oxidative stress response that occurs during spore inactivation, SOD activity levels

were tested. The results, which are shown in Figure 5c, exhibited the same change trend as that of CAT. In addition, rising intracellular ROSs can lead to cellular lipid oxidation and protein destruction. Therefore, compared with the other samples, the protein concentration in the spores was tested to have the largest decrease in protein (Figure 5d), which caused irreversible damage to the spores. The initial increase in CAT activity suggested that spores were also initially under $\cdot SO_4^-$ stress in the Vis/NS/PS system. As a result, an up-regulation of intracellular oxidative stress leads to the subsequent complete destruction of spores.

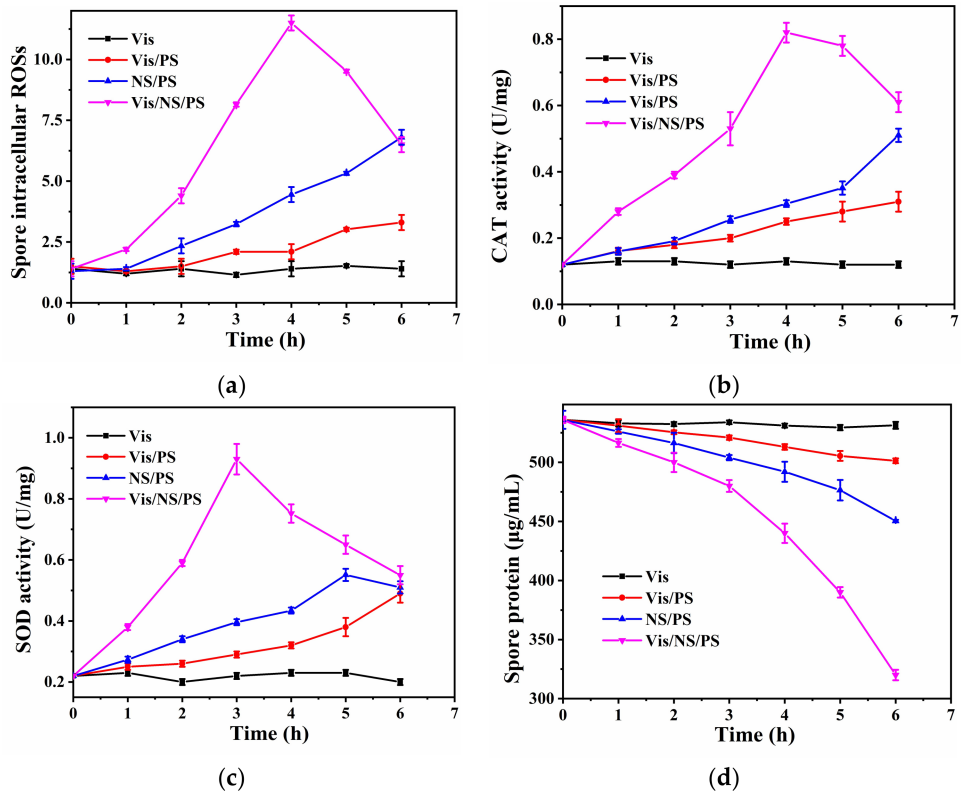

Figure 5. (**a**) Intracellular ROSs; (**b**) CAT activity; (**c**) SOD activity and (**d**) Protein concentration levels of bacteria spore in different treatment systems.

In order to more intuitively illustrate the inactivation process of spores in the Vis/NS/PS system, SEM tests were carried out on the samples at different times in the Vis/NS/PS system. As shown in Figure 6, oval bacterial spores possessed a pleated outer shell at 0 h. Over time, the epidermis of bacterial spores at 2 h and 4 h gradually became saturated due to the absorption of water by the core. Finally, the shells of bacterial spores ruptured at 5 h due to the violent attack of $\cdot SO_4^-$ and ·OH. Results of SEM characterization intuitively demonstrated the whole process of cell membrane damage and spore death under the action of strong oxidative stress in the Vis/NS/PS system.

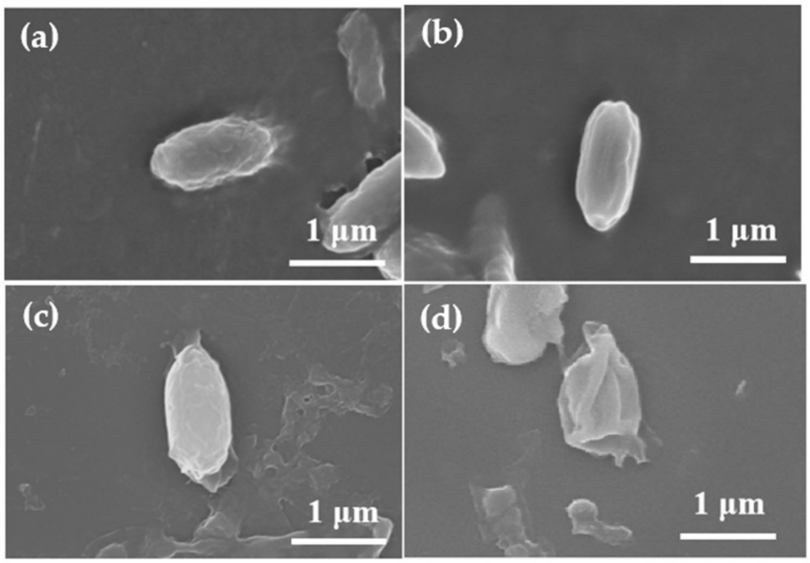

Figure 6. SEM images of *B. subtilis* spore treated by the Vis/NS/PS system with different irradiation time (Magnification: 20,000×). (**a**) 0 h, (**b**) 2 h, (**c**) 4 h, (**d**) 5 h.

Based on the above results, the overall mechanism of *B. subtilis* spore inactivation in the Vis/NS/PS system is illustrated in Figure 7. Firstly, NS was excited to generate photogenerated electrons, and $S_2O_8^{2-}$ was activated by photo-generated electrons to generate $\cdot SO_4^-$ in solution, then partially $\cdot SO_4^-$ converted to ·OH. Compared with ·OH, $\cdot SO_4^-$ has longer service life and stronger oxidation ability. Subsequently, free radicals, such as $\cdot SO_4^-$ and ·OH, penetrate the spore membrane to produce strong intracellular oxidative stress, resulting in up-regulation of the intracellular ROS level, further inducing high levels of CAT and SOD activity against adverse external environments. Finally, with the increase of ROS, the defense system was completely disrupted, resulting in damage to the cell membrane, leakage of cytoplasmic proteins, and spore death. These results provide a feasible method for inactivating spores in the field of water disinfection in the future.

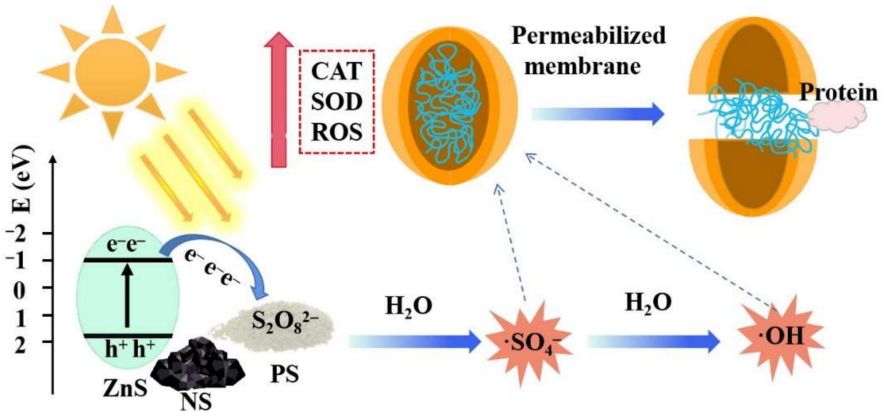

Figure 7. Graphical illustration of the bacterial spore inactivation mechanism in the Vis/NS/PS system.

4. Conclusions

In this study, the inactivation of bacterial spores using the Vis/NS/PS system was proposed for the first time. The NS was found to be natural metal-doped ZnS, which exhibited enhanced Vis absorption ability. To obtain pure spore, the effect of different ions on the sporulation efficiency was investigated, and Ca^{2+} was found to be more efficient than Mn^{2+} to obtain 100% sporulation. Under dark conditions, NS/PS system could inactivate 1.8 log of *B. subtilis* spores. In the Vis/NS/PS system, the inactivation effect of *B. subtilis* spores was significantly enhanced, which could completely inactivate 7 log of spore in 5 h.

The inactivation efficiency was four and seven times higher than that of NS/PS system and Vis/PS system, respectively. The inactivation efficiency was also positively associated with the light intensity and reaction temperature. The spore inactivation was initiated by the production of $\cdot SO_4^-$ and ·OH, leading to damage of the cell membrane as well as induction and destruction of anti-oxidant enzyme system. Since NS can be obtained with a large quantity without artificial synthesis, this work could provide useful information for developing alternative and "green" methods for the inactivation of bacterial spores, showing great potential in water disinfection with solar energy.

Supplementary Materials: The following supporting information can be downloaded at: https://www.mdpi.com/article/10.3390/coatings12040528/s1, Figure S1: The main metal ion concentration of NS (0.1 g/L) measured by ICP-MS after digesting NS with nitric acid; Figure S2: Sporulation efficiency of *B. subtilis* with different concentrations of Mn^{2+} after incubation at 37 °C for 8 days; Figure S3: (a–d) SEM images of *B. subtilis* cultured in NB medium supplemented with different concentrations of Ca^{2+} for 8 days; (e–h) SEM images of *B. subtilis* cultured in NB medium supplemented with different concentrations of Mn^{2+} for 8 days. In both cases, the cell density of produced spores was increased with the increase of metal ions (Magnification: 5000×); Table S1: Weight ratio of main metal component in NS.

Author Contributions: Writing—original draft preparation, formal analysis, investigation, Y.L.; methodology, validation, Z.L.; visualization, resources, D.L.; conceptualization, validation, writing—review and editing, supervision, W.W. All authors have read and agreed to the published version of the manuscript.

Funding: This research was funded by National Natural Science Foundation of China (No. 42122056), Guangdong Basic and Applied Basic Research Foundation (2021B1515020063), Science and Technology Program of Guangzhou, China (202002030177), National Key Research and Development Program of China (2019YFC1804501), Key Research and Development Program of Guangdong Province (2021B1111380003).

Institutional Review Board Statement: Not applicable.

Informed Consent Statement: Not applicable.

Data Availability Statement: The authors confirm that the data supporting the findings of this study are available within the article.

Conflicts of Interest: The authors declare no competing financial interest.

References

1. Dalrymple, O.K.; Stefanakos, E. A review of the mechanisms and modeling of photocatalytic disinfection. *Appl. Catal. B Environ.* **2010**, *98*, 27–38. [CrossRef]
2. Li, G.-Q.; Huo, Z.-Y. Synergistic effect of combined UV-LED and chlorine treatment on Bacillus subtilis spore inactivation. *Sci. Total Environ.* **2018**, *639*, 1233–1240. [CrossRef] [PubMed]
3. Makky, E.A.; Park, G.-S. Comparison of Fe (VI)(FeO42-) and ozone in inactivating Bacillus subtilis spores. *Chemosphere* **2011**, *83*, 1228–1233. [CrossRef] [PubMed]
4. Zeng, F.; Cao, S. Inactivation of chlorine-resistant bacterial spores in drinking water using UV irradiation, UV/Hydrogen peroxide and UV/Peroxymonosulfate: Efficiency and mechanism. *J. Clean. Prod.* **2020**, *243*, 118666. [CrossRef]
5. Luo, S.; Zhang, C. Photocatalytic water purification with graphitic C3N4-based composites: Enhancement, mechanisms, and performance. *Appl. Mater. Today* **2021**, *24*, 101118. [CrossRef]
6. Chen, R.; Li, J. Photocatalytic reaction mechanisms at the gas-solid interface for typical air pollutants decomposition. *J. Mater. Chem. A* **2021**, *9*, 20184–20210. [CrossRef]
7. Ge, J.; Zhang, Z. Photocatalytic degradation of (micro) plastics using TiO_2-based and other catalysts: Properties, influencing factor, and mechanism. *Environ. Res.* **2022**, 112729. [CrossRef]
8. Chen, Y.; Ng, T.W. Comparative study of visible-light-driven photocatalytic inactivation of two different wastewater bacteria by natural sphalerite. *Chem. Eng. J.* **2013**, *234*, 43–48. [CrossRef]
9. De Gutiérrez, R.M.; Villaquirán-Caicedo, M. Evaluation of the antibacterial activity of a geopolymer mortar based on metakaolin supplemented with TiO_2 and CuO particles using glass waste as fine aggregate. *Coatings* **2020**, *10*, 157. [CrossRef]
10. Tang, C.; Liu, C. Nontoxic carbon quantum dots/g-C3N4 for efficient photocatalytic inactivation of staphylococcus aureus under visible light. *Adv. Healthc. Mater.* **2019**, *8*, 1801534. [CrossRef]

11. Ghodsi, S.; Esrafili, A. Synthesis and application of g-C_3N_4/Fe_3O_4/Ag nanocomposite for the efficient photocatalytic inactivation of Escherichia coli and Bacillus subtilis bacteria in aqueous solutions. *AMB Express* **2021**, *11*, 1–12. [CrossRef] [PubMed]
12. Li, J.; Ma, R. Visible-Light-Driven Ag-Modified TiO_2 Thin Films Anchored on Bamboo Material with Antifungal Memory Activity against Aspergillus niger. *J. Fungi* **2021**, *7*, 592. [CrossRef] [PubMed]
13. Su, S.-F.; Ye, L.-M. Photoelectrocatalytic inactivation of Penicillium expansum spores on a Pt decorated TiO_2/activated carbon fiber photoelectrode in an all-solid-state photoelectrochemical cell. *Appl. Surf. Sci.* **2020**, *515*, 145964. [CrossRef]
14. Tang, X.; Tang, R. Application of natural minerals in photocatalytic degradation of organic pollutants: A review. *Sci. Total Environ.* **2021**, 152434. [CrossRef] [PubMed]
15. Li, G.; Chen, X. Natural sphalerite nanoparticles can accelerate horizontal transfer of plasmid-mediated antibiotic-resistance genes. *Environ. Int.* **2020**, *136*, 105497. [CrossRef] [PubMed]
16. Chen, Y.; Lu, A. Naturally occurring sphalerite as a novel cost-effective photocatalyst for bacterial disinfection under visible light. *Environ. Sci. Technol.* **2011**, *45*, 5689–5695. [CrossRef]
17. Moradi, M.; Kalantary, R.R. Visible light photocatalytic inactivation of Escherichia coli by natural pyrite assisted by oxalate at neutral pH. *J. Mol. Liq.* **2017**, *248*, 880–889. [CrossRef]
18. Peng, X.; Ng, T.W. Bacterial disinfection in a sunlight/visible-light-driven photocatalytic reactor by recyclable natural magnetic sphalerite. *Chemosphere* **2017**, *166*, 521–527. [CrossRef] [PubMed]
19. Wang, W.; Wang, H. Catalyst-free activation of persulfate by visible light for water disinfection: Efficiency and mechanisms. *Water Res.* **2019**, *157*, 106–118. [CrossRef]
20. Wang, W.; Wang, H. Visible light activation of persulfate by magnetic hydrochar for bacterial inactivation: Efficiency, recyclability and mechanisms. *Water Res.* **2020**, *176*, 115746. [CrossRef]
21. Latif, A.; Kai, S. Catalytic degradation of organic pollutants in Fe(III)/peroxymonosulfate (PMS) system: Performance, influencing factors, and pathway. *Environ. Sci. Pollut. Res.* **2019**, *26*, 36410–36422. [CrossRef] [PubMed]
22. Yang, X.; Li, Y. Photocatalytic reduction of carbon tetrachloride by natural sphalerite under visible light irradiation. *Sol. Energy Mater. Sol. Cells* **2011**, *95*, 1915–1921. [CrossRef]
23. Wu, D.; Wang, W. Visible-light-driven photocatalytic bacterial inactivation and the mechanism of zinc oxysulfide under LED light irradiation. *J. Mater. Chem. A* **2016**, *4*, 1052–1059. [CrossRef]
24. Kort, R.; O'brien, A.C. Assessment of heat resistance of bacterial spores from food product isolates by fluorescence monitoring of dipicolinic acid release. *Appl. Environ. Microbiol.* **2005**, *71*, 3556–3564. [CrossRef]
25. Karava, M.; Bracharz, F. Quantification and isolation of Bacillus subtilis spores using cell sorting and automated gating. *PLoS ONE* **2019**, *14*, e0219892. [CrossRef] [PubMed]
26. Kim, J.U.; Shahbaz, H.M. Inactivation of Bacillus cereus spores using a combined treatment of UV-TiO2 photocatalysis and high hydrostatic pressure. *Innov. Food Sci. Emerg. Technol.* **2021**, *70*, 102–116. [CrossRef]
27. Berberidou, C.; Paspaltsis, I. Heterogenous photocatalytic inactivation of B. stearothermophilus endospores in aqueous suspensions under artificial and solar irradiation. *Appl. Catal. B Environ.* **2012**, *125*, 375–382. [CrossRef]
28. Prasad, G.; Ramacharyulu, P. Photocatalytic inactivation of spores of Bacillus anthracis using titania nanomaterials. *J. Hazard. Mater.* **2011**, *185*, 977–982. [CrossRef]
29. Zacarías, S.M.; Vaccari, M.C. Effect of the radiation flux on the photocatalytic inactivation of spores of Bacillus subtilis. *J. Photochem. Photobiol. A Chem.* **2010**, *214*, 171–180. [CrossRef]
30. Fan, W.; Cui, J. Bactericidal efficiency and photochemical mechanisms of micro/nano bubble–enhanced visible light photocatalytic water disinfection. *Water Res.* **2021**, *203*, 117–131. [CrossRef]
31. Zacarías, S.M.; Manassero, A. Design and performance evaluation of a photocatalytic reactor for indoor air disinfection. *Environ. Sci. Pollut. Res.* **2021**, *28*, 23859–23867. [CrossRef] [PubMed]
32. Wang, W.; Xie, H. Visible Light-Induced Marine Bacterial Inactivation in Seawater by an In Situ Photo-Fenton System without Additional Oxidants: Implications for Ballast Water Sterilization. *ACS EST Water* **2021**, *1*, 1483–1494. [CrossRef]